JACS
JOURNAL OF THE AMERICAN CHEMICAL SOCIETY
Article
pubs.acs.org/JACS

Ultrafast Polarization Switching in a Biaxial Molecular Ferroelectric Thin Film: [Hdabco]ClO_4

Yuan-Yuan Tang,[†] Wan-Ying Zhang,[†] Peng-Fei Li,[†] Heng-Yun Ye, Yu-Meng You,* and Ren-Gen Xiong*

Ordered Matter Science Research Center, Southeast University, Nanjing 211189, People's Republic of China

Supporting Information

ABSTRACT: Molecular ferroelectrics are attracting much attention as valuable complements to conventional ceramic ferroelectrics owing to their solution processability and nontoxicity. Encouragingly, the recent discovery of a multiaxial molecular ferroelectric, tetraethylammonium perchlorate, is expected to be able to solve the problem that in the technologically relevant thin-film form uniaxial molecular ferroelectrics have been found to perform considerably more poorly than in bulk. However, it can show good polarization−electric field (P−E) hysteresis loops only at very low frequency, severely hampering practical applications such as ferroelectric random access memory. Here, we present a biaxial molecular ferroelectric thin film of [Hdabco]ClO_4 (dabco = 1,4-diazabicyclo[2.2.2]octane) (**1**), where a perfect ferroelectric hysteresis loop can be observed even at 10 kHz. It is the first example of a molecular ferroelectric thin film whose polarization can be switched at such a high frequency. Moreover, using piezoresponse force microscopy, we clearly observed the coexistence of 180° and non-180° ferroelectric domains and provided direct experimental proof that 180° ferroelectric switching and non-180° ferroelastic switching are both realized; that is, a flexible alteration of the polarization axis direction can occur in the thin film by applying an electric field. These results open a new avenue for applications of molecular ferroelectrics and will inspire further exploration of high-performance multiaxial molecular ferroelectric thin films.

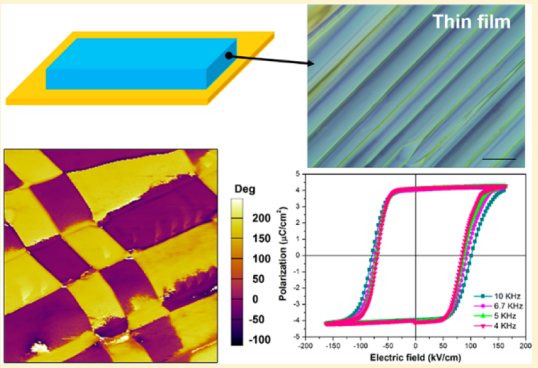

INTRODUCTION

Ferroelectric materials, where the spontaneous electric polarization can be reversed by electric field or mechanical force, have captured wide interest for technical applications such as ferroelectric random access memory (FeRAM), capacitors, ultrasound imaging, piezoelectric devices, and electro-optic materials for data storage.[1] The majority of commercial ferroelectrics so far belong to inorganic perovskite oxides, such as barium titanate (BTO) and lead zirconate titanate (PZT), although these materials contain heavy metals and usually require costly thermal vacuum processing.[2] As the alternative or the supplement, molecular ferroelectrics have been intensively studied to overcome the drawbacks because of their many advantages such as light weight, easy processing, mechanical flexibility, and environmental friendliness. Recently, many exciting advances have been achieved,[3] ranging from excellent ferroelectric properties, such as large spontaneous polarization up to 23 $\mu C/cm^2$ in croconic acid[3c] and diisopropylammonium bromide,[3b] high Curie temperature up to 426 K in diisopropylammonium bromide,[3b] to a novel ferroelectric mechanism, such as charge-transfer-induced ferroelectricity in organic cocrystals discovered by Stoddart and Stupp[3a] and recently discovered multiaxial ferroelectricity.[3f,4]

For miniaturization and integration, most ferroelectric materials are utilized in the form of thin film in applications such as microelectromechanical systems and FeRAM.[5] For molecular ferroelectrics, the research on the thin films is almost nonexistent. One of the reasons is because most molecular ferroelectrics are uniaxial with only two opposite polarization directions. The performance of the thin films of uniaxial ferroelectrics is usually not as good as that of the bulk crystals.[3f,4] Ferroelectric thin films are made of a very large number of variously oriented grains. If only one ferroelectric polar axis exists in a single-crystal grain, the sum of the spontaneous polarization vector of all the grains would be greatly reduced due to the randomly distributed polarization directions. Conversely, if molecular ferroelectrics are multiaxial ones with multiple equivalent polarization directions, like the inorganic ceramic ferroelectrics, a larger spontaneous polarization can be obtained in the corresponding polycrystalline sample after poling, allowing them to maintain excellent performance in the thin-film form.

Here, we show that ultrafast polarization switching can be realized in a biaxial molecular ferroelectric thin film of [Hdabco]ClO_4 (dabco = diazabicyclo[2.2.2]octane) (**1**), which was fabricated by a simple aqueous solution process. For the purpose of practical applications, polarization ordering and switching dynamics that are crucial to understand the

Received: October 9, 2016
Published: November 14, 2016

ACS Publications © 2016 American Chemical Society

DOI: 10.1021/jacs.6b10595
J. Am. Chem. Soc. 2016, 138, 15784−15789

physics of ferroelectrics should not be ignored.[6] Therefore, using piezoresponse force microscopy (PFM) and polarization *versus* electric field ($P-E$) hysteresis loop measurements, a systemic study for **1** was carried out at the microscopic and macroscopic scales. A very striking discovery is that the thin film of **1** can show a well-defined rectangular ferroelectric hysteresis loop even at a relatively high frequency of 10 kHz at room temperature. To our knowledge, the polarization switching at such a high frequency is unprecedented in molecular ferroelectric thin films. Even in the single-crystal form, many molecule-based ferroelectrics show the ferroelectric hysteresis loops only at very low frequencies,[7] such as croconic acid at 1 Hz,[3c] supramolecular charge-transfer cocrystals at about 1 Hz,[3a] and diisopropylammonium bromide at 25 Hz.[3b] Combining the multiple polarization directions and the ultrafast polarization switching, this system will pave the way toward practical applications in devices such as FeRAM.

RESULTS AND DISCUSSION

During our systematic search for multiaxial molecular ferroelectrics suitable for applications in the forms of thin films, we found that **1** crystallizes in the space groups $P4/mmm$ and $Pm2_1n$ at the high- and low-temperature phases, respectively. In view of the point group of the paraelectric phase, the number of the directions of spontaneous electric polarization in the low-temperature ferroelectric phase can be obtained as r, that is, $r = g_0/g$, where g_0 (*i.e.*, the order of point group G_0) represents the number of symmetry operations of point group G_0 of the high-temperature paraelectric phase and g (*i.e.*, the order of point group G) corresponds to the number of symmetry operations of point group G of the low-temperature ferroelectric phase. Thus, **1** belongs to the typical biaxial ferroelectric ($r = 16/4$).[3g] Although the preliminary investigation on the ferroelectricity of the single crystal of this material has been carried out, the properties of the polycrystalline samples have not been studied yet. Hence, we first conducted the variable-temperature dielectric constant measurement using a powder-pressed sample of **1**. In Figure S1, an obvious anomaly appears at about 377 K, consistent with the phase transition temperature in the previous report (also, the dielectric anisotropy of the single crystal of **1** can be found in Figure S1). The genuine characteristic of ferroelectricity was confirmed by the measurement of dielectric hysteresis loops using a powder sample of **1**. The polarization switching can be realized at 343 K using the Sawyer–Tower circuit method,[8] where the $P-E$ diagrams (Figure S2) show rectangular hysteresis loops at different frequencies. The powder-pressed pellet, which is the randomly oriented agglomerate of microcrystalline grains, can provide a $P-E$ hysteresis loop, suggesting the biaxial characteristic of **1** to some degree. The observed remnant polarization (P_r) is about 2.1 $\mu C/cm^2$. Unfortunately, the ferroelectric loops cannot completely open to reach saturation, and if the applied voltage is increased, the sample would be broken down. This behavior may result from the existence of a relatively large coercive field, E_c (which represents the minimum electric field demanded for switching the polarization).

In the event that the thickness of the sample is reduced by several orders of magnitude, a large electric field can be easily obtained with finite driving voltage. More importantly, the exploration of thin film would bring about potential device applications. Therefore, the thin film of **1** was prepared using a simple and inexpensive solution-based method. First, the pure powder of **1** was dissolved into deionized water to form a homogeneous aqueous precursor solution. Then a drop of the precursor solution was carefully deposited on a freshly cleaned ITO (indium tin oxide)-coated glass (conductive ITO was used as the bottom electrode). At 323 K, millimeter-scale dendritic crystals of **1** were neatly grown, and finally, a large-area, continuous film consisting of continuous dendritic crystals with high coverage was achieved. As shown in Figure 1, the film was

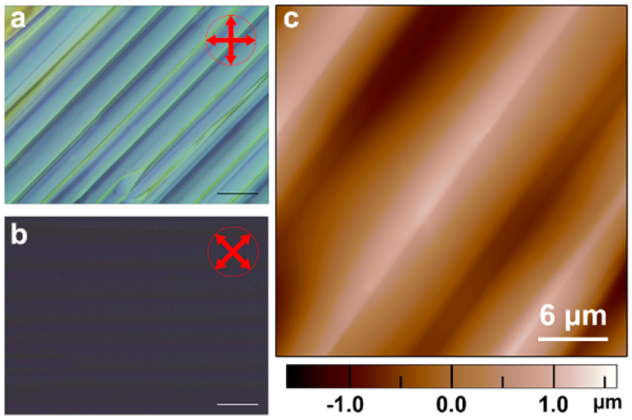

Figure 1. (a,b) Optical microscope photographs of thin film for **1** under crossed polarized light (scale bar: 20 um). (c) Atomic force microscopy images of the thin-film surface.

examined to be high quality under optical microscopy and atomic force microscopy. The inerratic allied dendritic crystals periodically in situ grew on the ITO-coated substrate without any visible pinholes. Under orthogonally polarized light, the homogeneous light intensity changes from bright to dark upon rotation around an axis perpendicular to the substrate, indicating that the film adopts an identical crystal orientation in the millimeter square range (Figures 1 and S3). Moreover, the packing views along the a-axis show the head-to-tail one-dimensional hydrogen-bonded chains along the c-axis through the N–H···N interactions between the adjacent $dabcoH^+$ cations (Figure S4). Hence, the c-axis should be parallel to the growing direction of dendritic crystals. Meanwhile, in-plane and out-of-plane X-ray diffractions have been performed for the thin film of **1** to exactly determine the molecular orientation. As shown in Figure S5, the major out-of-plane diffractions are (110), (020), (200), and (130), and the major in-plane diffraction is (001), demonstrating that the [001]-directional hydrogen bond does lie in the plane of the substrate.

To this high-quality thin film deposited on a conducting substrate, a drop of liquid GaIn eutectic was used as the top electrode to form a capacitor architecture (GaIn/thin film/ITO). The ferroelectric hysteresis loop measurements were then carried out with a commercial Sawyer–Tower circuit (Premier II ferroelectric tester). Excitingly, a perfect ferroelectric hysteresis loop can be obtained at a frequency as high as 10 kHz at room temperature (Figure 2). Such a high polarization switching in the thin film of **1** would pave the way toward the application in FeRAM. Most of molecular ferroelectrics can be operated at frequencies not more than 500 Hz.[7] The coercive electric voltage is about 25 V for a 3 μm thick film, corresponding to a coercive field of 83 kV/cm, smaller than those of the ferroelectric poly(vinylidene) difluoride family (~500 kV/cm).[9] The large P_r (remanent polarization) values, about 4 $\mu C/cm^2$, are comparable to that of the classical molecular ferroelectric crystals, such as triglycine

DOI: 10.1021/jacs.6b10595
J. Am. Chem. Soc. 2016, 138, 15784–15789

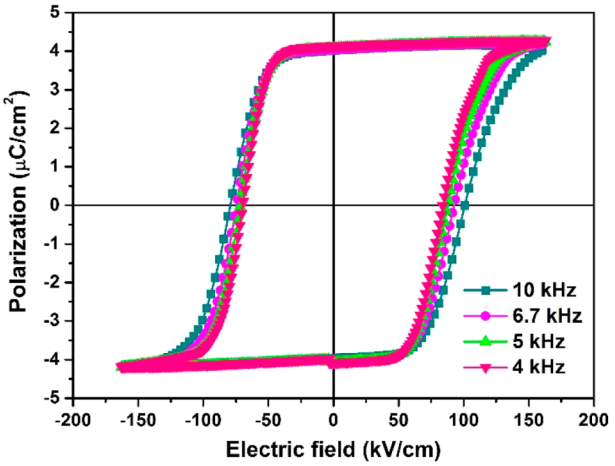

Figure 2. Room temperature ferroelectric hysteresis loops of the thin film of **1** at different AC frequencies.

sulfate (3.8 μC/cm^2).[9] Based on a point charge model, the calculated polarization is about 4.21 μC/cm^2, which reproduces the experimental value (see Table S1). Moreover, the P_r value almost remains unchanged upon increasing the frequency from 4 to 10 kHz, meaning that no significant attenuation occurs at high frequency. Many more measurements were carried out in the different regions of the thin film, and all can obtain the good hysteresis loop. This provides clear evidence that the ferroelectric polarization has a large component perpendicular to the substrate. In addition, the well-defined rectangular hysteresis loops can also be acquired on the different substrates, suggesting that the polarization switching performance of the thin film of **1** is unaffected by the substrate (the results are shown in Figure S6).

In order to investigate the microscopic ferroelectric polarization reversal, we carried out density functional calculations based on the Berry phase method developed by Kingsmith and Vanderbilt.[10] The first-principles calculations were performed within the framework of density functional theory implemented in the Vienna ab initio simulation package.[11] The energy cutoff for the expansion of the wave functions was fixed to 500 eV, and the exchange−correlation interactions were treated within the generalized gradient approximation of the Perdew−Burke−Ernzerhof type.[12] For the integrations over the *k*-space, we used a 3 × 3 × 5 *k*-point mesh. The experimental room temperature crystal structure[13] was used as the ground state for evaluating the ferroelectric polarization. The calculated polarization vector coincides with its crystallographic *b*-axis, which is in good agreement with the polar axis of the space group $Pm2_1n$. In order to further evaluate the magnitude of the ferroelectric polarization and the dynamic process of the polarization reversal, we consider the path connecting the center to the polar structure by linearly interpolating the atomic positions, which involves the relative displacement between the Hdabco cation and the perchlorate anion. The continuous evolution of spontaneous polarization from the centrosymmetric structure (λ = 0) to the polar structure (λ = 1) was plotted as a function of dimensionless structural parameter λ in Figure 3. From the curve, the estimated value of ferroelectric polarization is ∼5.68 μC/cm^2 in the polar state, which is contributed mainly by the displacement of the positive and negative centers.

From the crystallographic point of view, the twined multidomain state in a ferroelectric depends on the symmetry

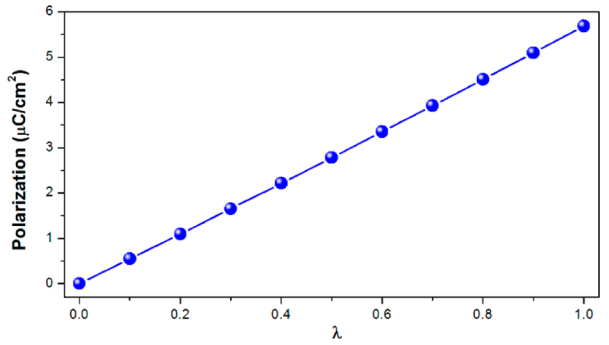

Figure 3. Polarization as a function of λ evaluated by density functional theory.

breaking from the paraelectric phase to the ferroelectric phase.[14] The resultant domain configuration is intrinsically decided by the spontaneous polarization direction in the ferroelectric phase and the symmetry of the corresponding paraelectric phase. Therefore, the angles of the symmetric equivalent directions in the paraelectric phase determine the specific angles between adjacent domains in the ferroelectric phase. For **1**, the ferroelectric phase adopts the space group $Pm2_1n$ (point group: *mm*2), whose polarization direction is confined to the [010]-direction by the crystallographic symmetry (Figure 4a). Taking into account its tetragonal paraelectric phase with the space group *P*4/*mmm* (point group: 4/*mmm*), the paraelectric-to-ferroelectric phase transition will result in the spontaneous polarization in the [110]-direction, which corresponds to the [010]-direction of its orthorhombic ferroelectric phase (Figure 4a). There are four symmetric equivalent directions in the paraelectric phase, so domains with 180 and 90° configuration can be expected to appear in the ferroelectric phase, like that in the tetragonal phase of BTO (Figure 4b). Furthermore, four polarization directions are all perpendicular to the *c*-axis. Considering that the *c*-axis is parallel to the grown direction of dendritic crystals, it is obvious that the ferroelectric polarization in any regions of the thin film has a component perpendicular to the substrate. In addition, due to the multiaxial characteristic, the component should be more than sin 45° times as big as the maximum saturation value after poling, thus guaranteeing the high performance in the thin-film form. On the other hand, this also explains why the hysteresis loop can be observed at any region.

To further confirm the thin-film ferroelectricity and the multiaxial characteristic, the thin films of **1** were investigated using PFM, which can provide nondestructive visualization of ferroelectric domains with ultrahigh spatial resolution.[15] The PFM amplitude reveals the relative strength of the piezoelectric coefficient, while the phase represents the direction of the polarization in each individual domain. Figure 5 presents the vertical PFM phase and amplitude images of the film surface for **1**. The PFM observation clearly demonstrates the stable domain structures in the annealed state, which is obtained by heating the sample to the paraelectric phase and then quickly cooling back to the ferroelectric phase. Figure 5a−d shows the similar domain patterns achieved from the two random places, meaning that these patterns exist almost everywhere. The formation of this aligned rectangle shape, among which two different domains are alternately arranged, mainly depends on the symmetry breaking upon the paraelectric-to-ferroelectric phase transition. The rich ∼90° angles between domain walls imply the potential presence of 90° domains, agreeing with the

DOI: 10.1021/jacs.6b10595
J. Am. Chem. Soc. 2016, 138, 15784−15789

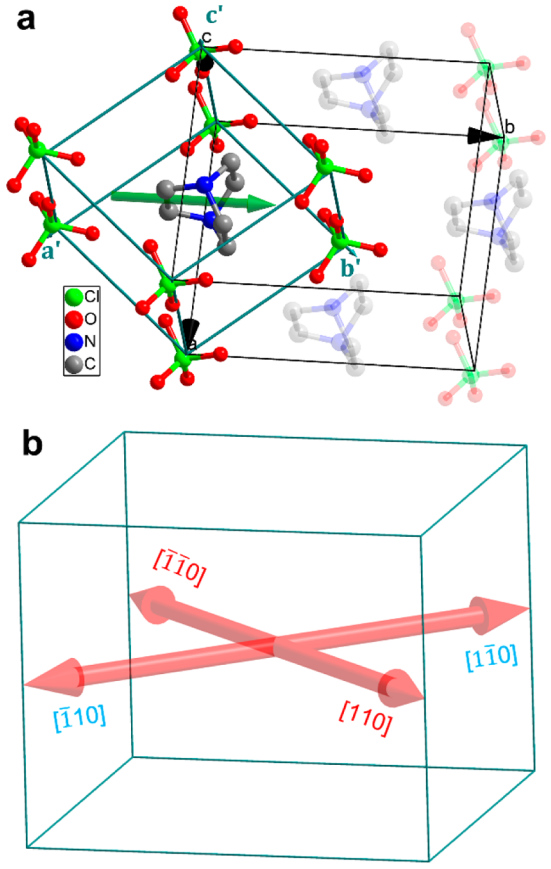

Figure 4. (a) Polarization direction of **1** (green arrow, [010]-direction) in the room temperature crystal cell (outlined in black solid lines). This direction coincides with the [110]-direction of its tetragonal paraelectric phase unit cell (outlined in green solid lines). (b) Four possible equivalent polarization directions of **1** in the ferroelectric phase.

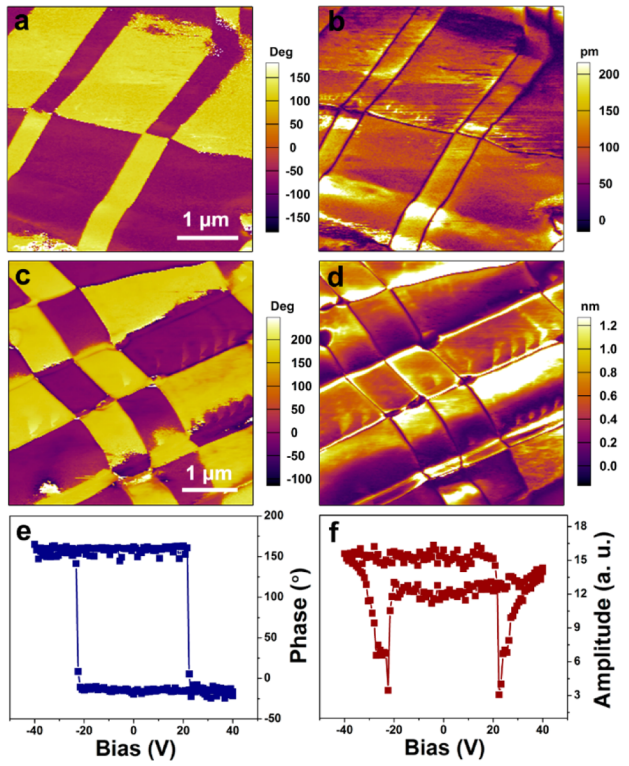

Figure 5. Vertical PFM phase (a,c) and amplitude images (b,d) for the thin film of **1**. (e,f) Phase and amplitude signals as functions of the tip voltage for a selected point, showing local PFM hysteresis loops.

above estimation of the polarization direction and manifesting the existence of multiple polar axes.

The most important features for ferroelectric materials is the electrically switchable spontaneous polarization, which describes the phenomenon of switching among several spontaneously polarized states under sufficiently large electrical load. Local PFM-based hysteresis loop measurement was carried out on the thin-film sample of **1** by applying an AC electric field superimposed on a DC triangle sawtooth waveform. The obvious 180° reversal of the PFM phase signal and the characteristic butterfly loop of the amplitude signal are typical for the switching of ferroelectric domains (Figure 5e,f). The local coercive voltages for a selected point are about +22.0 and −22.0 V, as indicated by the minima of the amplitude loop. In order to more intuitively observe the polarization switching process, we performed local switching tests by applying a large DC voltage between the conductive tip and ITO substrate. Figure 6 depicts results of an experiment aimed at poling the ferroelectric domains in the thin film of **1**.

We first scan the vertical PFM signals of the as-grown state over an area of 25 × 25 μm^2, revealing a typical stripe-like domain structure (Figure 6a). The phase image shows two domains with a clear contrast, which coincide with the regions of significant contrast in the amplitude image. When the phase signals are extracted to analyze, it can be found that the phase difference between two domains is close to 160°, but not 180°, as clearly shown in Figure S7a. Combined with the different strengths between two domains in the amplitude image, we guess that these domain walls should be non-180° domain walls. Subsequently, when a tip under −40 V bias was used to scan the thin-film surface, the polarization direction of the region marked by a blue box is switched (Figure 6b). In the phase image, two new colors appear in the reversed regions, meaning there are four phase contrasts now. From the statistical phase information, one can see that two new phase contrasts have 180° phase differences with the original two phase contrasts (Figure S7b). Also, given that the stripe-like domain pattern has almost no change, the switching should be 180° ferroelectric switching in this region under the electric load, thus validating the coexistence of 180° and non-180° domains in this film. Significantly, once an opposite +40 V bias is applied to the tip, the polarization orientation of the center region can be switched back and the box-in-box domain pattern forms, as the phase contrasts in the center region become the same with the outmost region (Figure 6c).

When the applied bias is increased to −60 V, the stripe-like domain pattern can also be wiped off; that is, non-180° ferroelastic switching occurs in the region marked by the red box, providing direct experimental proof for a flexible alteration of the polarization axis direction in the thin film by applying an electric field. As shown in Figure 6d, the piezoresponse in this region becomes almost homogeneous in both phase and amplitude images, revealing that the polarization state of this area is switched to the single-domain state. Moreover, the polarization in this domain can be switched back again by applying an opposite bias +35 V (Figure 6e). It should be noted that the topographic image of the same area of the film, obtained after these procedures, does not show any traces of

DOI: 10.1021/jacs.6b10595
J. Am. Chem. Soc. 2016, 138, 15784−15789

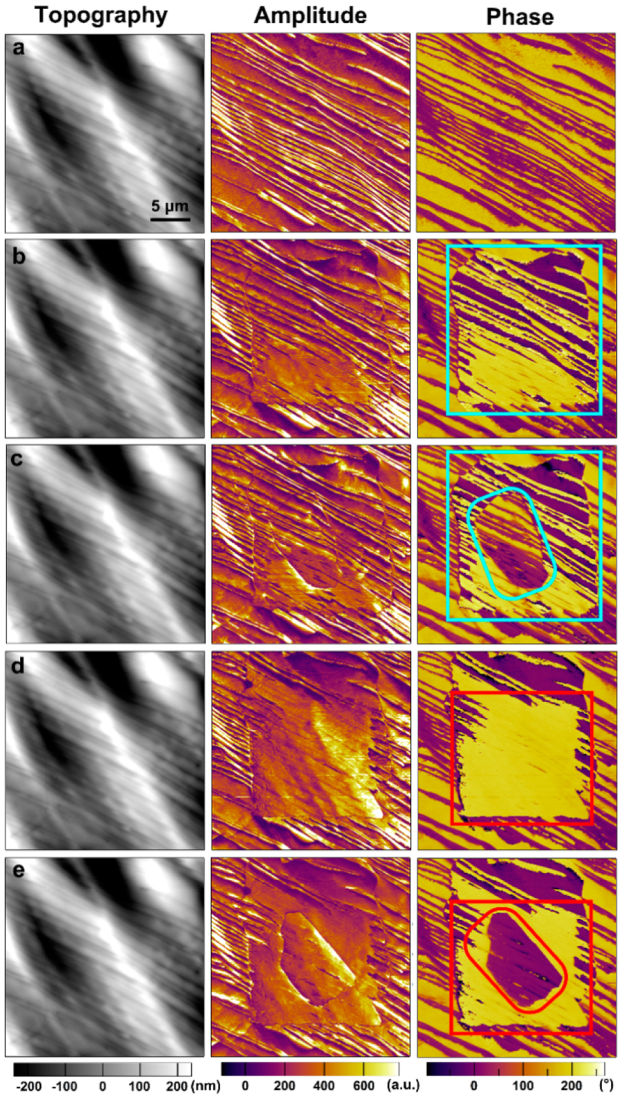

Figure 6. Panels in each column are arranged as the following sequence: topographic images (left), vertical PFM amplitude (middle), and last phase (right) images of the film surface. (a) Initial state. (b) After the first switching produced by scanning with the tip bias of −40 V. (c) After the succeeding back-switching produced by scanning with the tip bias of +40 V. (d) After the third switching produced by scanning with the tip bias of −60 V. (e) After the succeeding back-switching produced by scanning with the tip bias of +35 V.

surface deformation. The PFM results present strong evidence for the switchable and stable polarization in the thin film of **1**, where the coexistence of 180° and non-180° domains is observed, and 180° ferroelectric switching and non-180° ferroelastic switching are both realized.

CONCLUSION

In summary, we present a biaxial molecular ferroelectric thin film of **1**, which was fabricated by a simple and effective aqueous solution process. The growth begins with organized dendritic crystals, which finally merge together to form a continuous film. The homogeneous light intensity under orthogonally polarized light reveals the same crystal orientation in the large area film (square millimeter level). With this high-quality thin film, the well-defined rectangular *P*–*E* hysteresis loops are successfully achieved even at 10 kHz. In addition, the measured spontaneous polarization is about 4 $\mu C/cm^2$, comparable to that of a classical molecular ferroelectric, such as triglycine sulfate (3.8 $\mu C/cm^2$). Combined with the crystallographic analysis and the oriented growth of the film, the *c*-axis should be parallel to the growth direction of dendritic crystals. Furthermore, four polarization directions are all perpendicular to the *c*-axis, so the component perpendicular to the substrate should be more than sin 45° times as big as the maximum saturation value after poling, ensuring the high performance in the thin-film form. Meanwhile, using PFM, we show unambiguously the coexistence of 180° and non-180° ferroelectric domains in high-quality thin films. We also present evidence for the reversible 180° ferroelectric switching and non-180° ferroelastic switching of the ferroelectric domains by poling with DC biases in the ferroelectric phase, confirming the alteration of multiple polarization axis directions. The excellent film-forming ability, the multiaxial characteristics, and the ultrafast polarization switching make them ideal candidates for applications in next-generation flexible electronics.

EXPERIMENTAL SECTION

Materials. All reagents and solvents in the syntheses were of reagent grade and used without further purification. **1** was prepared by slow evaporation of the ethanol solution of dabco and $HClO_4$ in a 1:1 molar ratio. The powder of **1** was dissolved in purified water to form a solution with a solubility of about 100 mg/mL. With this solution, thin films were deposited on ITO-coated glass substrates.

Measurements. Nanoscale polarization imaging and local switching spectroscopy were carried out using a resonant-enhanced piezoresponse force microscopy (MFP-3D, Asylum Research). Conductive Pt/Ir-coated silicon probes (EFM-50, Nanoworld) were used for domain imaging and polarization switching studies. Resonant-enhanced PFM mode was applied to enhance the signal, with a typical AC voltage of 2.0 V at ~378 kHz.

ASSOCIATED CONTENT

Supporting Information

The Supporting Information is available free of charge on the ACS Publications website at DOI: 10.1021/jacs.6b10595.

Figures S1−S7, Table S1, and discussion (PDF)

AUTHOR INFORMATION

Corresponding Authors

*youyumeng@seu.edu.cn

*xiongrg@seu.edu.cn

ORCID

Ren-Gen Xiong: 0000-0003-2364-0193

Author Contributions

†Y.-Y.T., W.-Y.Z., and P.-F.L. contributed equally to this work.

Notes

The authors declare no competing financial interest.

ACKNOWLEDGMENTS

This work was supported by the 973 project (2014CB932103) and the National Natural Science Foundation of China (21290172, 91222101, and 21371032).

REFERENCES

(1) Lines, M. E.; Glass, A. M. *Principles and Applications of Ferroelectrics and Related Materials*; Clarendon Press: Oxford, UK, 1977.

(2) (a) Scott, J. F. *Science* **2007**, *315*, 954. (b) Scott, J. F.; Paz de Araujo, C. *Science* **1989**, *246*, 1400.

DOI: 10.1021/jacs.6b10595
J. Am. Chem. Soc. 2016, 138, 15784−15789

(3) (a) Tayi, A. S.; Shveyd, A. K.; Sue, A. C.; Szarko, J. M.; Rolczynski, B. S.; Cao, D.; Kennedy, T. J.; Sarjeant, A. A.; Stern, C. L.; Paxton, W. F.; Wu, W.; Dey, S. K.; Fahrenbach, A. C.; Guest, J. R.; Mohseni, H.; Chen, L. X.; Wang, K. L.; Stoddart, J. F.; Stupp, S. I. *Nature* **2012**, *488*, 485. (b) Fu, D. W.; Cai, H. L.; Liu, Y.; Ye, Q.; Zhang, W.; Zhang, Y.; Chen, X. Y.; Giovannetti, G.; Capone, M.; Li, J.; Xiong, R. G. *Science* **2013**, *339*, 425. (c) Horiuchi, S.; Tokunaga, Y.; Giovannetti, G.; Picozzi, S.; Itoh, H.; Shimano, R.; Kumai, R.; Tokura, Y. *Nature* **2010**, *463*, 789. (d) Tayi, A. S.; Kaeser, A.; Matsumoto, M.; Aida, T.; Stupp, S. I. *Nat. Chem.* **2015**, *7*, 281−294. (e) Sato, O. *Nat. Chem.* **2016**, *8*, 644. (f) Harada, J.; Shimojo, T.; Oyamaguchi, H.; Hasegawa, H.; Takahashi, Y.; Satomi, K.; Suzuki, Y.; Kawamata, J.; Inabe, T. *Nat. Chem.* **2016**, *8*, 946. (g) Katrusiak, A.; Szafrański, M. *Phys. Rev. Lett.* **1999**, *82*, 576. (h) Yao, Z. S.; Yamamoto, K.; Cai, H. L.; Takahashi, K.; Sato, O. *J. Am. Chem. Soc.* **2016**, *138*, 12005. (i) Xu, G. C.; Zhang, W.; Ma, X. M.; Chen, Y. H.; Zhang, L.; Cai, H. L.; Wang, Z. M.; Xiong, R. G.; Gao, S. *J. Am. Chem. Soc.* **2011**, *133*, 14948. (j) Ye, H. Y.; Zhou, Q.; Niu, X.; Liao, W. Q.; Fu, D. W.; Zhang, Y.; You, Y. M.; Wang, J.; Chen, Z. N.; Xiong, R. G. *J. Am. Chem. Soc.* **2015**, *137*, 13148.

(4) Ye, H.-Y.; Ge, J.-Z.; Tang, Y.-Y.; Li, P.-F.; Zhang, Y.; You, Y.-M.; Xiong, R.-G. *J. Am. Chem. Soc.* **2016**, *138*, 13175.

(5) (a) Wang, J.; Neaton, J.; Zheng, H.; Nagarajan, V.; Ogale, S.; Liu, B.; Viehland, D.; Vaithyanathan, V.; Schlom, D.; Waghmare, U. *Science* **2003**, *299*, 1719. (b) Zhang, Y.; Liu, Y.; Ye, H. Y.; Fu, D. W.; Gao, W.; Ma, H.; Liu, Z.; Liu, Y.; Zhang, W.; Li, J.; Yuan, G. L.; Xiong, R. G. *Angew. Chem., Int. Ed.* **2014**, *53*, 5064. (c) Gao, W.; Chang, L.; Ma, H.; You, L.; Yin, J.; Liu, J.; Liu, Z.; Wang, J.; Yuan, G. *NPG Asia Mater.* **2015**, *7*, e189. (d) Noda, Y.; Yamada, T.; Kobayashi, K.; Kumai, R.; Horiuchi, S.; Kagawa, F.; Hasegawa, T. *Adv. Mater.* **2015**, *27*, 6475.

(6) Lu, H.; Li, T.; Poddar, S.; Goit, O.; Lipatov, A.; Sinitskii, A.; Ducharme, S.; Gruverman, A. *Adv. Mater.* **2015**, *27*, 7832.

(7) (a) Zhang, W.; Chen, L. Z.; Xiong, R. G.; Nakamura, T.; Huang, S. D. *J. Am. Chem. Soc.* **2009**, *131*, 12544. (b) Zhang, W.; Ye, H.-Y.; Cai, H.-L.; Ge, J.-Z.; Xiong, R.-G.; Huang, S. D. *J. Am. Chem. Soc.* **2010**, *132*, 7300. (c) Szafrański, M. *Phys. Rev. B: Condens. Matter Mater. Phys.* **2005**, *72*, 054122. (d) Szafrański, M.; Katrusiak, A. *Phys. Rev. B: Condens. Matter Mater. Phys.* **2006**, *73*, 134111. (e) Sun, Z.; Chen, T.; Luo, J.; Hong, M. *Angew. Chem., Int. Ed.* **2012**, *51*, 3871. (f) Horiuchi, S.; Ishii, F.; Kumai, R.; Okimoto, Y.; Tachibana, H.; Nagaosa, N.; Tokura, Y. *Nat. Mater.* **2005**, *4*, 163. (g) Akutagawa, T.; Koshinaka, H.; Sato, D.; Takeda, S.; Noro, S.; Takahashi, H.; Kumai, R.; Tokura, Y.; Nakamura, T. *Nat. Mater.* **2009**, *8*, 342. (h) Jakubas, R.; Piecha, A.; Pietraszko, A.; Bator, G. *Phys. Rev. B: Condens. Matter Mater. Phys.* **2005**, *72*, 104107. (i) Zhang, Y.; Liao, W. Q.; Fu, D. W.; Ye, H. Y.; Chen, Z. N.; Xiong, R. G. *J. Am. Chem. Soc.* **2015**, *137*, 4928.

(8) Sawyer, C. B.; Tower, C. *Phys. Rev.* **1930**, *35*, 269.

(9) Horiuchi, S.; Tokura, Y. *Nat. Mater.* **2008**, *7*, 357.

(10) (a) Kingsmith, R. D.; Vanderbilt, D. *Phys. Rev. B: Condens. Matter Mater. Phys.* **1993**, *47*, 1651. (b) Vanderbilt, D.; Kingsmith, R. D. *Phys. Rev. B: Condens. Matter Mater. Phys.* **1993**, *48*, 4442.

(11) (a) Kresse, G.; Furthmuller, J. *Phys. Rev. B: Condens. Matter Mater. Phys.* **1996**, *54*, 11169. (b) Kresse, G.; Furthmuller, J. *Comput. Mater. Sci.* **1996**, *6*, 15.

(12) Perdew, J. P.; Burke, K.; Ernzerhof, M. *Phys. Rev. Lett.* **1996**, *77*, 3865.

(13) Olejniczak, A.; Anioła, M.; Szafrański, M.; Budzianowski, A.; Katrusiak, A. *Cryst. Growth Des.* **2013**, *13*, 2872.

(14) Shi, P.-P.; Tang, Y.-Y.; Li, P.-F.; Liao, W.-Q.; Wang, Z.-X.; Ye, Q.; Xiong, R.-G. *Chem. Soc. Rev.* **2016**, *45*, 3811.

(15) (a) Lee, D.; Lu, H.; Gu, Y.; Choi, S.-Y.; Li, S.-D.; Ryu, S.; Paudel, T. R.; Song, K.; Mikheev, E.; Lee, S.; Stemmer, S.; Tenne, D. A.; Oh, S. H.; Tsymbal, E. Y.; Wu, X.; Chen, L.-Q.; Gruverman, A.; Eom, C. B. *Science* **2015**, *349*, 1314. (b) Lu, H.; Bark, C. W.; Esque de los Ojos, D.; Alcala, J.; Eom, C. B.; Catalan, G.; Gruverman, A. *Science* **2012**, *336*, 59. (c) Garcia, V.; Fusil, S.; Bouzehouane, K.; Enouz-Vedrenne, S.; Mathur, N. D.; Barthelemy, A.; Bibes, M. *Nature* **2009**, *460*, 81. (d) Bonnell, D. A.; Kalinin, S. V.; Kholkin, A.; Gruverman, A. *MRS Bull.* **2009**, *34*, 648. (e) Kalinin, S. V.; Rodriguez, B. J.; Jesse, S.; Karapetian, E.; Mirman, B.; Eliseev, E. A.; Morozovska, A. N. *Annu. Rev. Mater. Res.* **2007**, *37*, 189. (f) Gruverman, A.; Auciello, O.; Tokumoto, H. *Annu. Rev. Mater. Sci.* **1998**, *28*, 101.

DOI: 10.1021/jacs.6b10595
J. Am. Chem. Soc. 2016, 138, 15784−15789